ISSN 1061-8309, Russian Journal of Nondestructive Testing, 2018, Vol. 54, No. 5, pp. 377–384. © Pleiades Publishing, Ltd., 2018.
Original Russian Text © A.V. Egorov, V.V. Polyakov, 2018, published in Defektoskopiya, 2018, No. 5, pp. 55–62.

ELECTROMAGNETIC METHODS

Eddy Current Testing of Metallic Materials Using Projection Methods

A. V. Egorov[a] and V. V. Polyakov[a, b, *]

[a]*Altai State University, Barnaul, 656049 Russia*
[b]*Institute of Strength Physics and Materials Science, Siberian Branch, Russian Academy of Sciences, Tomsk, 634055 Russia*
**e-mail: pvv@asu.ru*

Received June 6, 2017

Abstract—Using the example of nonmagnetic metallic materials, the projection methods of multidimensional analysis of multifrequency eddy-current testing measurement data presented for processing are considered. Based on the principal components method, the effects of electrical conductivity and sensor–material-surface gap on the results of testing have been separated. Using regression on principal components, the numerical values of the electrical conductivity and gap for manganese, copper, bronze, aluminum, and an aluminum alloy have been obtained. The results make it possible to extend the possibilities of nondestructive eddy-current evaluation of materials.

Keywords: eddy-current method, material evaluation, multidimensional data analysis, method of principal components

DOI: 10.1134/S1061830918050042

INTRODUCTION

The use of structural materials and articles made thereof under various mechanical and temperature actions requires the diagnostics and evaluation of their structure and physical characteristics. In this connection, of importance is the problem of developing new and refining existing methods for such diagnostics. For metallic materials, one of the most common nondestructive-testing techniques is the eddy-current method [1], which makes it possible to reveal various kinds of defects, first of all, cracks [2, 3]; determine their dimensions and locations; evaluate various physical characteristics [4]; monitor chemical composition and thermal treatment [5]; etc. At the same time, a disadvantage of this method is the fact that the result of eddy-current measurements is determined by the combined action of a large number of competing factors, including the physical properties of a material (chemical-composition–dependent electrical conductivity and magnetic permeability), the peculiarities of its structure, the type and sizes of flaws, the geometrical dimensions of particular samples or articles, and the parameters and modes of measurements being taken, first of all, the frequency of excited eddy currents and the gap between the sensor and the surface of an object being tested, as well as specific features of particular measuring devices and parameters of sensors being used. Depending on the particular problem being solved in eddy-current testing, one needs to single out the effect of one or another factor or of a group of factors, with all the other factors treated as interferences that one should get rid of.

This problem of separating certain factors and isolating parameters that are needed for a particular task can be solved with different approaches. One of the approaches is to develop dedicated designs of eddy-current transducers and measuring devices that have maximum sensitivity toward the parameter being tested. With this approach being associated with the increased complexity in manufacturing the probe, it still does not allow one to eliminate the influence of interfering factors completely. Another approach is based on using theoretical dependences of the probe parameters on the characteristics of the test object [6, 7] that eventually follow from the solution of the system of Maxwell equations. However, these dependences can be derived only for a rather small number of fairly artificial special cases.

In this paper, to separate competing factors that concurrently affect the results of eddy-current measurements, we propose to use the projection methods of multidimensional data analysis, which proved their efficiency when solving a wide range of tasks related to revealing hidden regularities under concurrent action of many factors [8, 9]. Using the example of nonmagnetic materials with different physical properties, we describe how to isolate separate factors with the method of principal components and also consider the possibilities offered by the proposed approach in quantitative estimation of these factors.

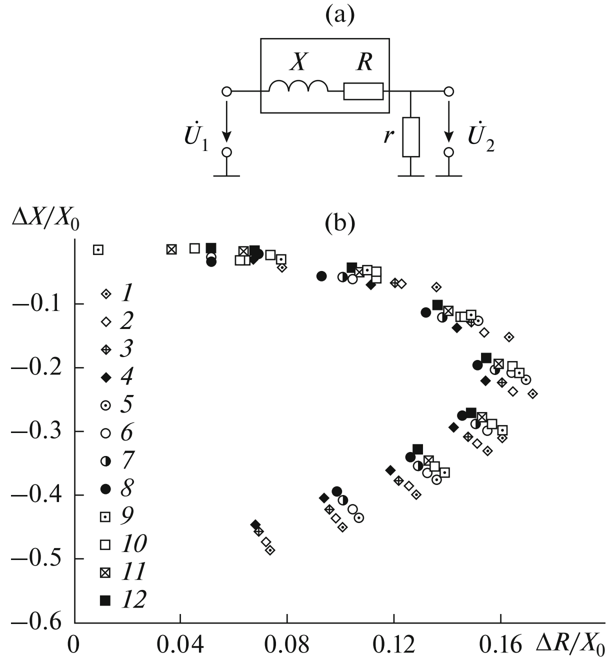

Fig. 1. Eddy-current measurements for copper, manganese, and bronze: (a) scheme of eddy-current measurements; (b) experimental hodographs for "sensor-sample" system. The gap values *h* are for copper (*1*) 0.07, (*2*) 0.10, (*3*) 0.14, (*4*) 0.20; for manganese (*5*) 0.07, (*6*) 0.10, (*7*) 0.14, (*8*) 0.20; and for bronze (*9*) 0.07, (*10*) 0.1, (*11*) 0.14, (*12*) 0.20 mm.

EXPERIMENTAL PROCEDURE AND MATERIALS

In eddy-current techniques that are based on measurements at a single fixed frequency, suppressing interfering factors presents an extremely complicated problem and, as a rule, is accomplished with the labor-intensive procedure of selecting an optimum measurement mode. The greatest information capacity of the eddy-current method is attained when using multifrequency measurements [10], which result in producing experimental hodographs for the sensor–test-sample system. The hodographs are constructed in a wide frequency range and reflect the combined action of virtually all factors that are of significance when evaluating the structure and properties of materials.

Tested articles can be of different dimensions and shapes, a fact that significantly narrows down the application domain of through-type sensors under real industrial conditions. Therefore, all measurements were taken with an attachable-type parametric 20-mm-in-diameter probe that was an induction coil with the core made of a manganese-nickel ferrite with relative initial magnetic permeability $\mu = 2000$. Eddy-current measurements were taken in a frequency band of 100–6400 Hz that sufficed for reliable construction of hodograph lines. In the present paper, we used multifrequency measurements in which the measurement error was reduced by processing the signals with Walsh functions [4, 11].

Materials were evaluated using the automated measuring-computing facility that determines the impedance of the induction probe [9]. A simplified measurement scheme that was used to determine impedance is depicted in Fig. 1a. It included a generator that shaped a sine-wave signal with the complex amplitude

$$\dot{U}_1 = U_1 e^{j\varphi_1},$$

where U_1 is the amplitude of the generator signal and φ_1 is its initial phase. This signal was fed through a measuring circuit that consisted of a gage sensor with a reactive resistance X and active resistance R as well as a resistor with resistance r that converted the current in the circuit into an alternating voltage with the complex amplitude

$$\dot{U}_2 = U_2 e^{j\varphi_2},$$

where U_2 is the signal amplitude and φ_2 is its initial phase. The two complex amplitudes $\dot{U}_1$ and $\dot{U}_2$ were related as

$$\dot{U}_2 = \frac{r}{r + R + jX}\dot{U}_1.$$

Equating the real and imaginary parts of this equality, we arrive at

$$\begin{cases}(r + R)U_2 = rU_1\cos(\varphi_1 - \varphi_2)\\ XU_2 = rU_1\sin(\varphi_1 - \varphi_2)\end{cases}.$$

a relation that entails, respectively, the following formulae for calculating the reactive X and active R probe resistances:

$$X = r\frac{U_1}{U_2}\sin(\varphi_1 - \varphi_2),$$

$$R = r\left[\frac{U_1}{U_2}\cos(\varphi_1 - \varphi_2) - 1\right].$$

The results of measurements were presented in the form of experimental hodographs, with relative changes in the probe's active resistance $\Delta R/X_0$ laid off as abscissas and relative changes in its active resistance $\Delta X/X_0$, as ordinates. Here, $\Delta R = R - R_0$ is the change in the probe's active resistance due to the sample; $\Delta X = \omega(L - L_0)$ is the change in its reactive resistance due to the sample; X_0, L_0, and R_0 are, respectively, the active resistance, inductance, and reactive resistance of the probe with no sample; and ω is the cyclic frequency of the input sine-wave signal.

Eddy-current tests were run on nonmagnetic metallic materials with different electrical conductivities σ for copper, manganese, bronze, aluminum, and an aluminum alloy. Tested samples were flat plates with dimensions 100 × 100 × 20 mm. The geometrical dimensions of the samples balanced out edge effects; the plate thickness exceeded the skin depth at the used frequencies. Testing for copper, manganese, and bronze was carried out in order to construct mathematical models and reveal specific features of the proposed approach, while aluminum and its alloy were involved to trial the method and investigate its capabilities.

The procedure of isolating one of the competing factors while eliminating other (interfering) factors was performed using the example of electrical conductivity and the gap between the attachable sensor and the sample surface. A gap h, which is one of the main interferences under real conditions, was created using dielectric spacers and varied from 0 to 1 mm. The electrical conductivities σ of studied samples were determined by the four-terminal sensing method to be 57 ± 5 MS/m (copper), 22 ± 2 (manganese), 8.5 ± 0.8 (bronze), 34 ± 4 (aluminum), and 16 ± 2 (D16T aluminum alloy). The eddy-current transducer pickup signal depended simultaneously on the electrical conductivity and the gap, thus allowing analysis of the capabilities of the proposed technique in separating competing factors.

Figure 1b presents the results of eddy-current measurements in the form of experimental hodographs in the $\Delta R/X_0 - \Delta X/X_0$ coordinates for copper, manganese, and bronze for four different gap values h. The measurements were taken at fixed frequencies of 100, 200, 400, 800, 1600, 3200, and 6400 Hz. It can be seen that the groups of points that describe different materials with different electrical conductivities but for the same gap value fall on one and the same curve. The effect of electrical conductivity was that as it increased, points from the upper part of the hodograph line, which corresponded to the lower frequencies, travelled to the lower part, which corresponded to the high frequency. Such behavior of the points was accounted for by the fact that their position on the hodograph line for a fixed gap value was only determined by the value of a generalized eddy-current parameter β, proportional to the product of electrical conductivity and frequency, $\beta \sim \sqrt{\omega\sigma}$. Hodograph lines obtained for one and the same material but different gap values were shifted with respect to each other. The shift was more noticeable in the lower part of the hodographs, corresponding to the range of higher frequencies.

Overall, the arrangement of experimental points in Fig. 1b shows that separating the influences of separate factors (in this case, electrical conductivity and gap value) on the examined characteristics based on the shape of the hodographs is difficult, with any quantitative estimation of the relevant parameters being virtually impossible. This indicates the necessity for developing methods that would provide such a possibility in eddy-current measurements.

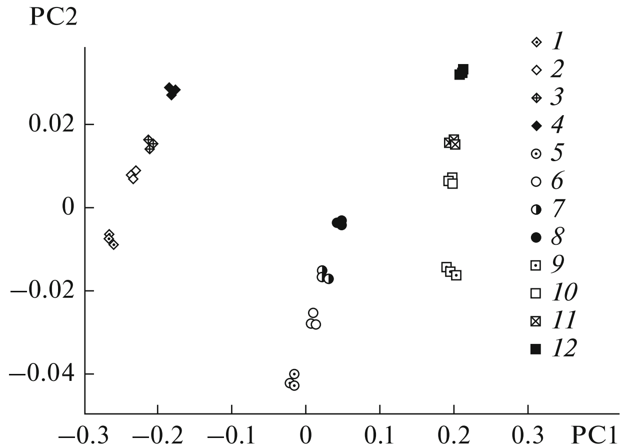

Fig. 2. Projections of eddy-current measurement results onto the plane of the first principal components. The gap values are for copper (*1*) 0.07, (*2*) 0.20, (*3*) 0.50, (*4*) 1.0; for manganese (*5*) 0.07, (*6*) 0.2, (*7*) 0.50, (*8*) 1.0; and for bronze (*9*) 0.07, (*10*) 0.20, (*11*) 0.50, (*12*) 1.0 mm.

APPLYING THE METHOD OF PRINCIPAL COMPONENTS TO SEPARATION OF INFLUENTIAL FACTORS

The method of principal components [8] was employed to separate factors affecting the results of eddy-current measurements. According to this method, the results of all measurements were treated as the coordinates of points in a multidimensional space. The totality of experimental data for a particular sample formed the so-called feature vector, which defined the position of a point in the multidimensional space. Points describing samples with close characteristics were located close to each other, in one domain of the multidimensional space. Hidden regularities in the results of measurements were revealed by switching to a new orthogonal coordinate system that was constructed so that its first axis (principal component PC1) pointed toward the maximum spread of experimental points; the second axis (principal component PC2), orthogonal with respect to the first one, toward the next-in-value spread of points; with other axes (principal components PC3 and so on) selected similarly. We used the projection of multidimensional experimental data onto the plane of the first principal components for pictorial representation and visual analysis of results.

The processing and analysis of the experimental hodographs consisted in the following. For the eddy-current measurements that were taken, the feature vector characterized the reaction of the parametric transducer (sensor) to the test sample [12]. The relative changes in the active $\Delta R(\omega_n)/X_0(\omega_n)$ and reactive $\Delta X(\omega_n)/X_0(\omega_n)$ resistances of the probe at the used fixed frequencies served as feature-vector coordinates. In such a manner, every sample, characterized by a particular value of electrical conductivity and a prescribed gap value, was described by one point in the $2n$-dimensional space, with its position defined by the feature vector that contained the coordinates of the experimental hodograph constructed based on n frequencies (in our case, $n = 7$). Testing itself was conducted for groups of samples, each including 10 samples with the same electrical conductivity and gap value. The data of the testing are presented in Fig. 2 as the graph of projections onto the plane of the first principal components PC1 and PC2. It can be seen that the points that characterize measurements for the same metal but with different gap values split into standalone groups situated on distinctly seen lines. Materials with different electrical conductivities were described by lines that were substantially spaced apart in the plane of the first principal components. This can be rephrased as that the PC1 axis in these graphs reflected, firs of all, separation of materials by their physical properties (the value of electrical conductivity) while the PC2 axis was mainly responsible for the specific features of the measurement mode (the value of the gap between the probe and material surface). It follows from the analysis of points in Fig. 2 that the method of principal components allowed a fairly reliable separation of the main factors affecting the results of eddy-current measurements.

APPLYING REGRESSION ON PRINCIPAL COMPONENTS TO QUANTITATIVE DETERMINATION OF TESTED CHARACTERISTICS

The method of regression on principal components [8] was used to quantitatively determine the values of electrical conductivity and gap based on the experimental hodographs resulting from eddy-current

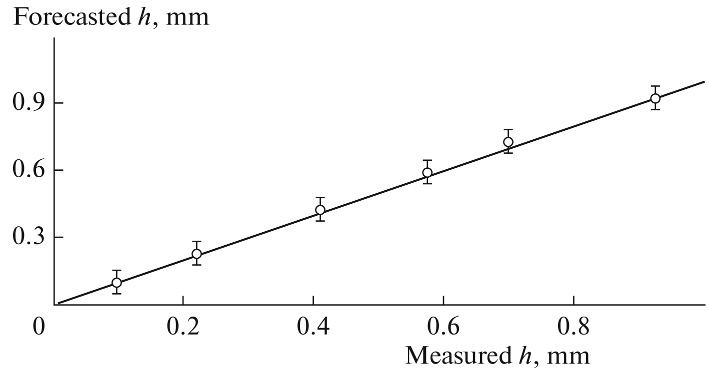

Fig. 3. Determining gap value.

measurements. This method is used when one knows the experimental relationship between the feature vector and those parameters of the test object that affect the coordinates of this vector. In this case, one can construct mathematical models that establish such a relationship. A two-stage procedure is used in the method of regression on principal components. At the first stage, the method of principal components is used to create a new coordinate system by the algorithm described in the previous section. At the second stage, a linear mathematical model is constructed that relates the test-object parameters h and σ with the coordinates t_i in the coordinate system transformed at the first stage in the form

$$h = a_0 + \sum_{i=1}^{m} a_i t_i,$$

$$\sigma = b_0 + \sum_{i=1}^{l} b_i t_i.$$

The weight coefficients a_i and b_i were selected based on the least root-mean-square deviation of the experimental points from the results of linear modeling. It should be noted that the number of coordinates l and m that are used in approximation is, as a rule, smaller than that of the original ones. This is connected with the fact that increasing the ordinal number of the coordinate axis leads to a drop in the effect of the tested parameters on the relevant coordinate, with this effect becoming comparable with the influence of random factors in measurements.

When constructing a regression model intended for determining the gap value, we used $m = 3$, while in the calculations, we employed the values of h determined from six independent measurements. The relevant experimental data comprised a calibration sampling, whereas relationships between feature vectors and measured parameters defined a calibration dependence, which was further used to forecast the gap value based on experimental hodographs. The results of calculations according to this model are displayed in Fig. 3. The theoretical values are shown as the straight line, and measurements for three metals are given as the points. The variance in the values of h, shown as a confidence interval, described the effect of electrical conductivity that served in this case as an interfering factor. The variance can be seen to be fairly small, i.e., the effect of electrical conductivity is insignificant.

The second model, aimed at forecasting the value of electrical conductivity, was constructed similarly, with the values of σ for copper, manganese, and bronze determined from independent measurements serving as tested parameters. The corresponding calibration dependence for $l = 5$ is shown in Fig. 4a, where the straight line reflects theoretical values and the points indicate experimental data for different gap values. The spread of these points around the straight line, which represents the variance in the values of electrical conductivity, is noticeably larger than in Fig. 3. This implies that the influence of gap value (playing the role of an interfering factor in the second model) is rather significant.

In order to improve the second model, its modification was proposed in which the interval of gap values was split into smaller segments and respective calibration curves were produced for every segment, with the original hodographs remaining unchanged. Five segments of equal length were used, viz., from 0 to 0.2, from 0.2 to 0.4, from 0.4 to 0.6, from 0.6 to 0.8, and from 0.8 to 1.0 mm. The results of calculations for five regression models constructed independently for each of the five segments are shown in Fig. 4b.

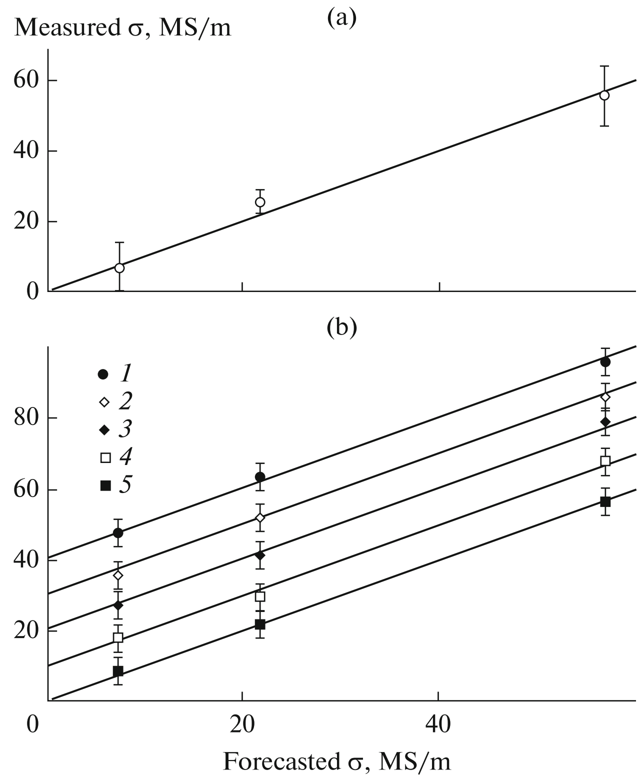

Fig. 4. Determining electrical conductivity: (a) gap value from 0 to 1 mm; (b) gap values (*1*) from 0 to 0.2 (forecasted value σ + 40 MS/m), (*2*) from 0.2 to 0.4 (σ + 30 MS/m), (*3*) from 0.4 to 0.6 (σ + 20 MS/m), (*4*) from 0.6 to 0.8 (σ + 10 MS/m), (*5*) from 0.8 to 1.0 mm.

It can be seen from the figure that we managed to considerably reduce the influence of gap and decrease the variance in the values of electrical conductivity.

In such a manner, the proposed approach to processing the results of multifrequency eddy-current testing makes use of an algorithm that includes the following sequence of actions.

1. Eddy-current measurements are performed for specially prepared samples with known electrical conductivities and gaps. Based on these measurements, a calibration table is compiled that includes the following data: electrical conductivities σ, gap thicknesses h (dictated by dielectric spacers), experimental values of $\Delta R(\omega_n)/X_0(\omega_n)$ and $\Delta X(\omega_n)/X_0(\omega_n)$ for a set of fixed frequencies.

2. The data in the thus-compiled table are processed using the iteration algorithm of the method of principal components [8], which translates the array of experimental data into a new coordinate system that makes it possible to separate interfering factors, in our case, electrical conductivities and gaps. The result of such separation can be pictorially represented as the graph of projections onto the selected coordinate axes (see Fig. 2).

3. Regression models are constructed for the values of gaps and electrical conductivities. These models are used to reveal the spread in forecasted values that affect the accuracy of determining the characteristics being computed.

4. Measurements for actual articles being tested are taken with the same set of frequencies as the one used when constructing the calibration table. Using the regression models produced at the previous stage, the unknown values of thicknesses h and electrical conductivities σ are calculated.

CALCULATING THE VALUES OF TESTED PARAMETERS FOR NONMAGNETIC MATERIALS

The calibration models constructed in the previous section were used to quantitatively determine the values of the gap and electrical conductivity for samples made of the same materials (copper, manganese, and bronze) but for the gap values that had not been used under calibration, i.e., for test samples with “unknown”

Table 1. Tested characteristics for copper, manganese, and bronze

Material	h, mm		σ, MS/m	
	measured	calculated	measured	calculated
Copper	0.14 ± 0.05	0.13	57 ± 6	57.1
	0.30 ± 0.05	0.31		58.45
	0.50 ± 0.05	0.50		57.3
	1.0 ± 0.1	0.99		55.3
Manganese	0.14 ± 0.05	0.12	22 ± 2	22.3
	0.30 ± 0.05	0.29		22.6
	0.50 ± 0.05	0.52		22.05
	1.0 ± 0.1	0.98		24.3
Bronze	0.14 ± 0.05	0.10	8.5 ± 0.8	7.8
	0.30 ± 0.05	0.31		8.8
	0.50 ± 0.05	0.53		7.9
	1.0 ± 0.1	0.99		8.6

Table 2. Tested characteristics for aluminum-based materials

Material	h, mm		σ, MS/m	
	measured	alculated	measured	alculated
Aluminum	0.14 ± 0.05	0.11	34 ± 4	34.3
	0.30 ± 0.05	0.32		35.0
	0.50 ± 0.05	0.51		35.6
	1.0 ± 0.1	0.97		34.8
D16T alloy	0.14 ± 0.05	0.09	16 ± 2	15.2
	0.30 ± 0.05	0.28		16.5
	0.50 ± 0.05	0.48		14.8
	1.0 ± 0.1	0.98		17.7

values of h and σ. The data obtained with the constructed regression models are compared with the independent measurements of h and σ in Table 1. It can be seen from the table that the computed values of gap and electrical conductivity coincide with the measured values to within the measurement error.

The above approach was additionally tested on aluminum and D16T aluminum alloy, materials with considerably different electrical conductivities that had not participated in the construction of the models. This enhanced the reliability of approbation for both the constructed calibration models and the proposed method itself. The forecasted and measured values of h and σ for aluminum and D16T-aluminum-alloy samples are provided in Table 2. Comparing these values to each other also indicates a rather high accuracy that can be achieved when determining the tested characteristics.

CONCLUSIONS

The analysis of the results has shown that the method of principal components allows reliable separation of competing factors affecting the results of eddy-current testing. This can be used, for example, when grading samples of materials with unknown chemical composition without resorting to labor-intensive chemical analysis; when revealing the influence of previous thermal or mechanical treatment; when classifying materials by their properties; and in other tasks of the kind. Applying regression on principal components made it possible to determine, quantitatively and with a high degree of accuracy, the values of tested characteristics based on the results of eddy-current measurements. The mathematical models developed within the framework of the proposed approach are important when designing new techniques for eddy-current evaluation of the structure and composition of materials and articles. These models can be successfully employed in the problem of nondestructive thickness gaging of dielectric coatings on metals with arbitrary and a priori unknown composition.

Thus, applying the projection methods of multidimensional analysis to the results of eddy-current measurements allows one to considerably extend the possibilities of nondestructive eddy-current testing.

ACKNOWLEDGMENTS

This work was supported by the Russian Foundation for Basic Research, project no. 17-08-00914.

REFERENCES

1. *Nerazrushayushchii kontrol'. Spravochnik. V 7t* (Nondestructive Testing. A Handbook. 7 vols.) Klyuev, V.V., Ed., Moscow: Mashinostroenie, 2003.
2. Garcia-Martin, J., Gomez-Gil, J., and Vazquez-Sanchez, E., Non-destructive techniques based on eddy current testing, *Sensors (Basel)*, 2011, vol. 11(3), pp. 2525–2565.
3. Yang, H.C. and Tai, C.C., Pulsed eddy-current measurement of a conducting coating on a magnetic metal plate, *Meas. Sci. Technol.*, 2002, vol. 13, pp. 1259–1265.
4. Egorov, A.V., Polyakov, V.V., Salita, D.S., et al., Inspection of aluminum alloys by a multi-frequency eddy current method, *Defence Technol.*, 2015, vol. 11, pp. 99–103.
5. Bakunov, A.S., Muzhitskii, V.F., and Shubochkin, S.E., A modern solution to problems of eddy-current structuroscopy, *Russ. J. Nondestr. Test.*, 2004, vol. 40, no. 5, pp. 346–349.
6. Yakimov, E.V., Urazbekov, E.I., Gol'dshtein, A.E., and Bulgakov, V.F., Computational transformation of signals of a measuring information system for eddy-current flaw detection, *Russ. J. Nondestr. Test.*, 2013, vol. 49, no. 11, pp. 657–663.
7. Dyakin, V.V. and Sandovskii, V.A., *Teoriya i raschet nakladnykh vikhretokovykh preobrazovatelei* (Theory and Calculation of Attachable Eddy-Current Transducers), Moscow: Nauka, 1981.
8. Esbensen, K., *Analiz mnogomernykh dannykh. Izbrannye glavy* (Analysis of Multidimensional Data. Selected Chapters), Kucheryavskii, S.V., Transl., Chernogolovka: Inst. Probl. Chem. Phys., Russ. Acad. Sci., 2005.
9. Egorov, A.V. and Polyakov, V.V., The application of principal-component analysis during eddy-current testing of aluminum alloys, *Russ. J. Nondestr. Test.*, 2015, vol. 51, no. 10, pp. 633–638.
10. Shokralla, S., Morelli, J.E., and Krause, T.W., Principal components analysis of multifrequency eddy current data used to measure pressure tube to calandria tube gap, *IEEE Sensors J.*, 2016, vol. 16, no. 9, pp. 3147–3154.
11. Zalmanzon, L.A., *Preobrazovaniya Fur'e, Uolsha, Khaara i ikh primenenie v upravlenii, svyazi i drugikh oblastyakh* (Fourier, Walsh, and Haar Transforms and Their Applications in Control, Communication, and Other Fields), Moscow: Nauka, 1989.
12. Egorov, A.V., Kucheryavskiy, S.V., and Polyakov, V.V., Resolution of effects in multi-frequency eddy current data for reliable diagnostics of conductive materials, *Chemom. Intell. Lab. Syst.*, 2017, vol. 160, pp. 8–12.

Translated by V. Potapchouck